INL/CON-08-13821
PREPRINT

Implications of Air Ingress Induced by Density-Difference Driven Stratified Flow

ICAPP 2008

Chang Oh
Eung Soo Kim
Richard Schultz
David Petti
C. P. Liou

June 2008

The INL is a
U.S. Department of Energy
National Laboratory
operated by
Battelle Energy Alliance

This is a preprint of a paper intended for publication in a journal or proceedings. Since changes may be made before publication, this preprint should not be cited or reproduced without permission of the author. This document was prepared as an account of work sponsored by an agency of the United States Government. Neither the United States Government nor any agency thereof, or any of their employees, makes any warranty, expressed or implied, or assumes any legal liability or responsibility for any third party's use, or the results of such use, of any information, apparatus, product or process disclosed in this report, or represents that its use by such third party would not infringe privately owned rights. The views expressed in this paper are not necessarily those of the United States Government or the sponsoring agency.

Proceedings of ICAPP '08
Anaheim, CA USA, June 8-12, 2008
Paper 8023

IMPLICATIONS OF AIR INGRESS INDUCED BY DENSITY-DIFFERENCE DRIVEN STRATIFIED FLOW

Chang Oh, Eung Soo Kim, Richard Schultz, and David Petti
Idaho National Laboratory
P.O. Box 1625
Idaho Falls, ID 83415
Tel:208-526-7716 , Fax:208-526-0528, Email:Chang.Oh@inl.gov

C. P. Liou
University of Idaho
Moscow, ID 83844

Abstract – *One of the design basis accidents for the Next Generation Nuclear Plant (NGNP), a high temperature gas-cooled reactor, is air ingress subsequent to a pipe break. Following a postulated double-ended guillotine break in the hot duct, and the subsequent depressurization to nearly reactor cavity pressure levels, air present in the reactor cavity will enter the reactor vessel via density-gradient-driven-stratified flow. Because of the significantly higher molecular weight and lower initial temperature of the reactor cavity air-helium mixture, in contrast to the helium in the reactor vessel, the air-helium mixture in the cavity always has a larger density than the helium discharging from the reactor vessel through the break into the reactor cavity. In the later stages of the helium blowdown, the momentum of the helium flow decreases sufficiently for the heavier cavity air-helium mixture to intrude into the reactor vessel lower plenum through the lower portion of the break. Once it has entered, the heavier gas will pool at the bottom of the lower plenum. From there it will move upwards into the core via diffusion and density-gradient effects that stem from heating the air-helium mixture and from the pressure differences between the reactor cavity and the reactor vessel. This scenario (considering density-gradient-driven stratified flow) is considerably different from the heretofore commonly used scenario that attributes movement of air into the reactor vessel and from thence to the core region via diffusion. When density-gradient-driven stratified flow is considered as a contributing phenomena for air ingress into the reactor vessel, the following factors contribute to a much earlier natural circulation-phase in the reactor vessel: (a) density-gradient-driven stratified flow is a much more rapid mechanism (at least one order of magnitude) for moving air into the reactor vessel lower plenum than diffusion, and consequently, (b) the diffusion dominated phase begins with a much larger flow area and a much shorter distance for air to move into the core than earlier scenarios that attribute all air ingress from the reactor cavity into the core to diffusion only. Hence, consideration of the density-gradient-driven stratified flow phenomena will likely lead to more rapid air ingress into the core and also the presence of more air for core graphite oxidation than the widely-used air ingress attributed solely to diffusion.*

This paper discusses the density-gradient-driven stratified flow phenomena and the implications of considering this behavior on the progression of the air ingress event. Preliminary calculations are used to underline the importance of considering the density-gradient driven stratified flow phenomena in subsequent validation experiments and software development for analyzing VHTR scenarios.

I. INTRODUCTION

The U.S. Department of Energy is working through the Idaho National Laboratory to explore the potential for a Next Generation Nuclear Plant (NGNP)[1] based on the Very High Temperature Gas-Cooled Reactor (VHTR). The candidate system may be either a pebble-bed or a prismatic, graphite-moderated thermal neutron-spectrum reactor using helium as the working fluid. Presently the reactor outlet temperature has not been specified. However, dependent on the NGNP mission, the design average outlet temperature may be as high as 950 ºC (1223 K).

Because the NGNP may be used to generate process heat an intermediate heat exchanger will likely be a part of the primary system. Also, because the NGNP will likely be used to generate electricity, the plant may be either a

direct-cycle or an indirect cycle system. The Brayton cycle may be used to generate electricity. The reactor will be designed to ensure passive decay heat removal without fuel damage throughout the accident envelope.

The basic technology for the NGNP has been established in former high-temperature gas-cooled reactor plants (e.g., DRAGON, Peach Bottom, Albeitsgemeinschaft Versuchsreaktor [AVR], Thorium Hochtemperatur Reaktor [THTR], and Fort St. Vrain [2]). These reactor designs represent the two design categories: the pebble bed reactor and the prismatic modular reactor. Commercial examples of potential NGNP candidates are the Gas Turbine-Modular Helium Reactor (GT-MHR) from General Atomics [3], the High Temperature Reactor concept from AREVA [4], and the Pebble Bed Modular Reactor (PBMR) from the PBMR consortium [5]. Furthermore, the Japanese High-Temperature Engineering Test Reactor (HTTR) and the Chinese High-Temperature Reactor (HTR-10) are demonstrating the feasibility of the reactor components and materials needed for the NGNP. (The HTTR achieved a maximum average coolant outlet temperature of 950°C (1223 K) in April, 2004.) Therefore, the NGNP program is focused on building a plant to publicly demonstrate the safety and economics of the VHTR, rather than simply confirming the basic feasibility of the concept.

II. BACKGROUND

The potential for air ingress into the VHTR vessel stems from consideration of postulated loss-of-coolant-accidents (LOCAs). Since the VHTR is located in a reactor cavity that is filled with air under normal operational conditions, if a LOCA occurs then air may be given the opportunity to move into the reactor vessel. It is presently thought that the worst-case scenario will occur if a double-ended guillotine break is postulated in the hot duct. The hot duct is a large pipe (exact dimensions presently not defined—but the outer diameter is over a meter) that connects the reactor vessel with the vessel housing the power conversion system.

For a double-ended guillotine rupture, the transient will commence with a depressurization from operating pressure (assumed to be approximately 7 to 9 MPa) as helium is discharged into the reactor cavity. During the depressurization phase hot helium from the vessel will mix with the air in the reactor cavity. Hence a helium-laced air mixture will be available to move into the reactor vessel once the break is unchoked and the flow behavior at the break changes from momentum-driven flow from the reactor vessel into the reactor cavity to density-gradient driven stratified countercurrent flow with helium moving into the reactor cavity and helium-laced air moving into the reactor vessel from the reactor cavity.

The potential for density-gradient governed stratified air ingress into the VHTR following a large-break LOCA was first described in the NGNP Methods Technical Program Plan [1] based on stratified flow studies performed with liquid [6, 7]. Studies on density-gradient driven stratified flow in advanced reactor systems have been the subject of active research for well over a decade since density-gradient dominated stratified flow is an inherent characteristic of passive systems used in advanced reactors.

The work done on Generation 3+ systems, although for light water reactors, is conceptually identical and directly applicable to describe the phenomenological behavior that occurs in the NGNP. Even though the earlier studies were based on Generation 3+ systems using water as the working fluid, the governing equations are identical. The boundary conditions change to reflect the differences in the working fluid and the reactor vessel geometry. Recently a simple computational fluid dynamic calculation was made to mimic the LOCA between two tanks filled with helium and oxygen, respectively. The scenario is depicted in Fig. 1.

Earlier studies of the mechanisms leading to air ingress into the reactor vessel were focused on diffusion as described by Fick's Law [8 to 14]and ignored the effects of density-gradients on the interactions between helium (low density) and air or helium-laced air (high density) flow.

Air ingress into the reactor vessel stemming from density-gradient driven stratified flow occurs in a much quicker time scale than diffusion and results in a depressurized conduction cooling scenario with a different set of boundary conditions than previously assumed. Hence experiments are needed to study these phenomena as noted in the NGNP Methods Thermal-Fluids Experiment Plan [15] to supplement earlier work [6. 7, 16]. Subsequent to the break in the hot duct hypothesized in the depressurized conduction cooldown scenario, air present in the reactor cavity will enter the reactor vessel and because of the significantly higher molecular weight and lower initial temperature of the reactor cavity air, the air-helium mixture in the cavity is always heavier than the helium discharging from the reactor vessel through the break into the reactor cavity. Once the air-helium mixture enters the reactor vessel, it will pool at the bottom of the lower plenum. From the lower plenum the air will move into the core via diffusion and density-gradients induced by heating and the pressure differences between the reactor cavity and the reactor vessel. When density-gradient-driven stratified flow is considered as a contributing phenomena for air

ingress into the reactor vessel, the following factors contribute to a much earlier natural circulation-phase in the reactor vessel: (a) density-gradient-driven stratified flow is a much more rapid mechanism (at least one order of magnitude) for moving air into the reactor vessel lower plenum than diffusion, and consequently, (b) the diffusion dominated phase begins with a much larger flow area and a much shorter distance for air to move into the core than earlier scenarios that attribute all air ingress from the reactor cavity into the core to diffusion alone. Finally, the relative pressures between the reactor vessel and the reactor cavity will induce air movement until an equilibrium condition is achieved.

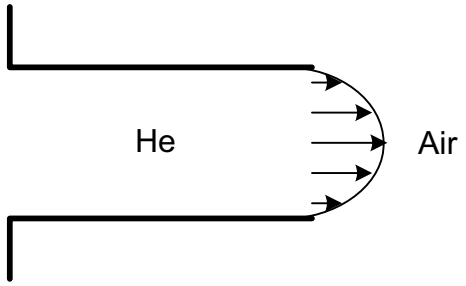

Figure 1 (a). Depressurization.

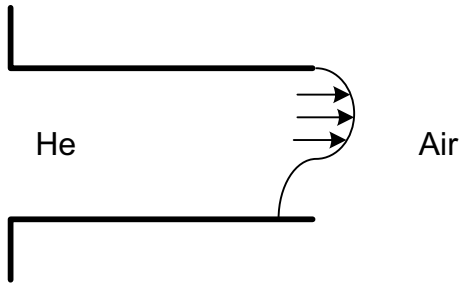

Figure 1 (b). Onset of density driven flow (no flow at the bottom of the break).

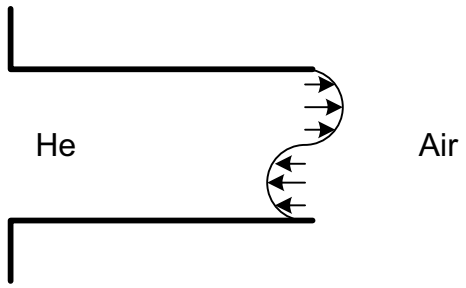

Figure 1 (c). Density driven flow (Reverse flow at the bottom of the pipe).

In essence the stratified flow assumption is based on the formation of a wedge of air in the lower portion of the hot duct break which will advance into the reactor vessel as a function of the density-gradients when the blowdown has become unchoked. Such flows are well characterized by the densimetric Froude number F which correlates the densities of helium and the air mixture to a constant value representative of the flow condition at different times in the scenario.

$$F = \frac{u}{\sqrt{g' d}} \tag{1}$$

in which u = discharge velocity of air, d = hydraulic depth of air, and g' = reduced gravity defined by

$$g' = \frac{g(\rho_2 - \rho_1)}{\frac{\rho_2 + \rho_1}{2}} \tag{2}$$

The buoyancy induced by the density difference of the two fluids necessitates the usage of reduced gravity g' instead of the standard gravity g. The magnitude of F indicates the magnitude of inertia force relative to the buoyancy created by stratification, and is a controlling parameter in stratified flows. This idea and experimental confirmation can be found in Liou et al. [6] and Yih [16].

A stratified flow experiment is required to better understand the phenomenon, to provide data for computational fluid dynamics (CFD) code validation since CFD codes will be used in conjunction with systems analysis codes to model this inherently multi-dimensional phenomenon. It is expected the densimetric Froude number will be found to be a function of

$$F = f\left(\alpha, L/D, \frac{V_{vessel}}{V_{vault}}, P_R, R\right) \tag{3}$$

in which α = orientation of the break with respect to the vertical, L = length of the separated hot duct on the reactor vessel side, D = diameter of the hot duct, V = volume, Pr = Pressure coefficient, and R = Reynolds number.

Thus, as shown in Figure 1(a), outward flow of helium into the reactor cavity from the reactor vessel continues until the reactor pressure is sufficiently reduced such that the blowdown flow first becomes unchoked. Thereafter, air starts to intrude into the pipe through the lower portion of the break as depicted in Figs. 1(b) and 1(c). In a rectangular flow cross section, it can be shown theoretically that the volumetric flow rate of the two fluids through the break are the same [6]. We therefore assume that the helium volumetric flow and air volumetric flow are equal. The heavy air will enter the vessel and collected (allowing turbulent mixing) at the bottom of the VHTR and air will penetrate the VHTR lower plenum and the

core through diffusion and thermally-induced density gradients. Ultimately these phenomena will induce natural circulation in the reactor, resulting in graphite oxidation. The graphite oxidation will be detrimental to the VHTR safety. If the stratified air flow induces the natural circulation flow to begin earlier than previously thought, then the time frame for graphite oxidation will occur earlier, and will likely occur at a more rapid rate. Earlier predictions from the GAMMA code [17] predict oxidation between 150 - 200 hours following pipe rupture, depending on the initial air volume in the containment. Calculations using MELCOR predict that oxidation begins at 220 hours [17] following pipe rupture. FLUENT [18] calculations, using the stratified flow approach presented in this paper, predict that natural circulation commences earlier than 150 hours. Hence the need to clarify our understanding of this phenomena and its effect on the progression of the scenario are quite important.

III. PROBLEM DESCRIPTION

Preliminary calculations were conducted to estimate the air ingress that stems from density-gradient driven stratified flow. A short description of the underlying assumptions is given below. The commercial CFD code FLUENT [18] is being used to model the hot duct and reactor vessel of the GT-MHR 600 MWt [19]—a General Atomic, Inc. design with a prismatic core. Figure 2 shows the reactor configuration.

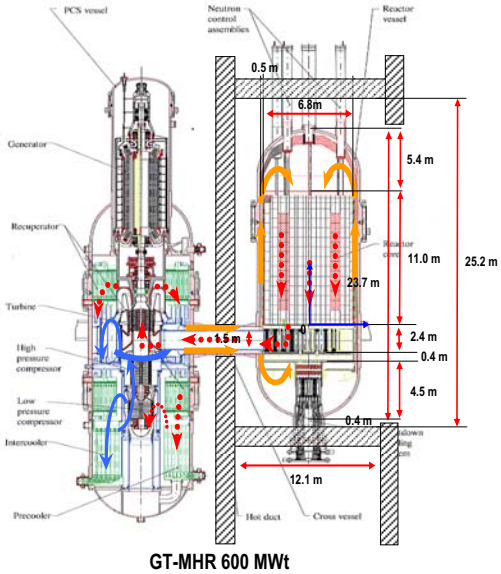

Figure 2. GT-MHR 600 MW_t.

For the first simulation the reactor core was simplified because the detailed geometry of the reactor is too complicated to be modeled rigorously. For simplification, the core, reflector and lower plenum were considered as porous bodies. The simplified geometry is illustrated in Figure 3. The flow path between the cavity and the core includes the break via the hot duct. The fluid region was divided into 5 parts. Zone 5 represents the reactor cavity. Zone 4 represents the portion of the reactor vessel excluding the core and hot duct. Zone 3 presents the hot duct, Zone 2 represents the lower plenum, and Zone 1 represents the core. Zones 1 and 2 are modeled as porous media while zones 3, 4, and 5 are non-porous media.

Realizable k-ε model was selected as a turbulence model. This model generally shows more improved predictions for the complicated flow such as high streamline curvature, transitional flow, rotation and recirculation than the standard k-ε model.

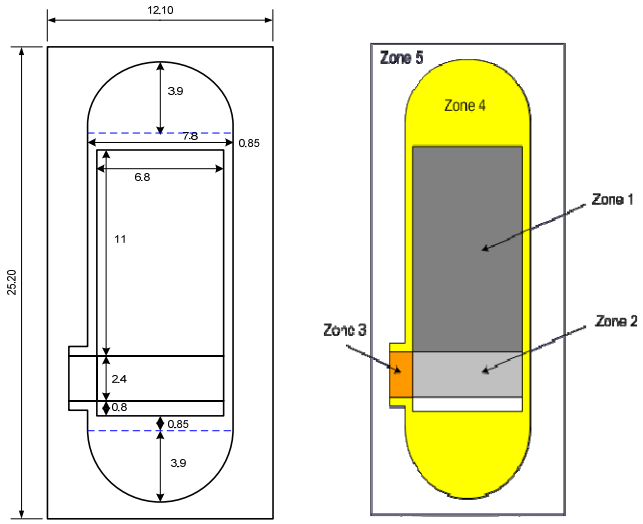

Figure 3. Simplified 2-D geometry for GT-MHR 600 MWt.

For the first calculation, the non-iterative time-advancement (NITA) scheme available in FLUENT was used. The traditional iterative time-advancement scheme requires a considerable amount of computational time due to a large number of outer iterations performed for each time-step. Because the NITA scheme does not use outer iterations, the transient calculations are considerably quicker.

Operating Boundary and Initial Conditions: For the calculations, the operating pressure was set equal to 1 atm (101325 Pa) in all the fluid zones. Two gas species: air and helium, were considered. The detailed mixture model is summarized as follows:

- Mixture species : air / helium

- Density model : incompressible ideal gas
- Heat capacity : mass weighted
- Thermal conductivity : mass weighted
- Viscosity : kinetic theory
- Mass diffusion : constant dilute approximation

The property model of each species was set using the National Institute of Science and Technology (NIST) chemistry webbook [20].

Porous Body Parameters: The porous media are modeled by the addition of a momentum source term to the standard fluid equation. The source term is composed of two parts: a viscous loss term (Darcy, the first term), and an inertial loss term.

$$S_i = -\left(\sum_{j=1}^{3} D_{ij} \mu \, v_j + \sum_{j=1}^{3} C_{ij} \frac{1}{2} \rho \, v_{mag} v_j \right) \quad (4)$$

where S_i is the source term for the ith (x, y, or z) momentum equation, D_{ij} and C_{jj} are the viscous loss coefficient matrices and the inertia loss coefficient matrices, respectively to calculate the pressure gradient in the porous media.

To recover the case of simple homogeneous porous media

$$S_i = -\left(\frac{\mu}{\alpha} v_i + C_2 \frac{1}{2} \rho \, v_{mag} v_i \right) \quad (5)$$

where α is the permeability and C_2 is the inertial resistance factor, simply specify D_{ii} and C_{jj} as diagonal matrices with $1/\alpha$ and C_2, respectively, on the diagonals (and zero for the other elements). V_{mag} is the magnitude of local superficial velocity.

FLUENT also allows the source term to be modeled as a power law of the velocity magnitude:

$$S_i = -C_0 |v|^{C_1} \quad (6)$$

where C_0 and C_1 are user-defined empirical coefficients.

Two important parameters define the porous media: porosity and permeability. The process to determine these parameters for the reactor core and the lower plenum is described in the following paragraphs:

<u>*Porosity:*</u> The porosity is the volume fraction equal to the fluid volume over the total volume (where the total volume equals the fluid volume plus the structural volume) of the region in question. The porosity is used in the calculation of the heat transfer in the medium and in the time-derivative term in the scalar transport equations for unsteady flow. It also influences the calculation of the reaction source terms and body forces in the medium. These sources will be proportional to the fluid volume in the medium.

In this study, two porosities were defined: the reactor core and the lower plenum. Figure 4 shows a typical VHTR reactor core block. The porosity of the core zone is

$$\gamma_{core} = \frac{V_{fluid}}{V_{total}} = \frac{A_{fluid}}{A_{total}} = \frac{\frac{1}{8}\pi d^2}{\frac{\sqrt{3}}{4} p^2} \quad (7)$$

and the porosity of the lower plenum, based on the geometry shown in Figures 5 and 6 is

$$\gamma_{lowerplenum} = \frac{V_{fluid}}{V_{total}} = \frac{A_{fluid}}{A_{total}} = \frac{\frac{\sqrt{3}}{4} p_{LP}^{\,2} - \frac{1}{8}\pi d_{LP}^{\,2}}{\frac{\sqrt{3}}{4} p_{LP}^{\,2}} \quad (8)$$

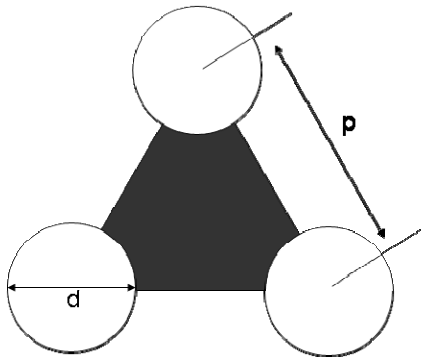

Figure 4. Core pattern (d = 1.58 cm, p = 3.27 cm).

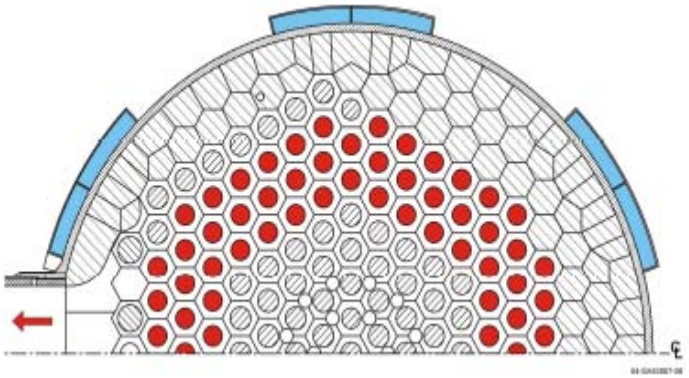

Figure 5. Typical geometry of lower plenum (d = 0.212 m, p = 0.36 m) [21].

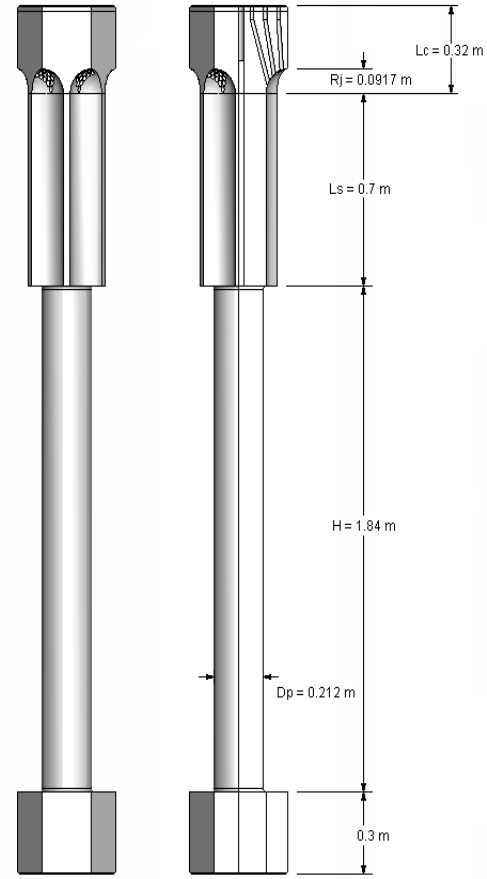

Figure 6. Detail view of lower plenum in GT-MHR 600 MWt.

From the above equations, the porosities of the reactor core and the lower plenum were calculated to be 0.21 and 0.68 respectively: :

Permeability: The permeability of the porous media model is a measure of the flow conductance of the porous media. In this study the permeability was calculated in the horizontal (x-direction) and vertical (y-direction) for both the reactor core and the lower plenum. The core and the lower plenum regions were treated differently.

The stratified flow in the lower plenum will occur with very hot helium passing over confinement-temperature air. Although the stratified flow is density-driven, the density gradients will be influenced by the large temperature differences in addition to the inherent density differences that exist between helium and air. Consequently, the temperature and gas specie-driven density gradients will be large and the flow will likely be turbulent.

The flow from the lower plenum into the core will be driven by concentration-driven diffusion and the buoyancy imparted to the air by localized heating. Because these density gradients will be low, the flow will likely be laminar.

A. Reactor core: The permeability in the vertical direction was determined by adapting the relationships for circular pipe flow. Figure 7 shows the friction factor as a function of Reynolds number, as expressed in the Moody diagram for a smooth pipe, where the Reynolds number is defined in terms of pipe diameter. The pipe diameter is correlated to the porous media using hydraulic diameter for packed spheres.

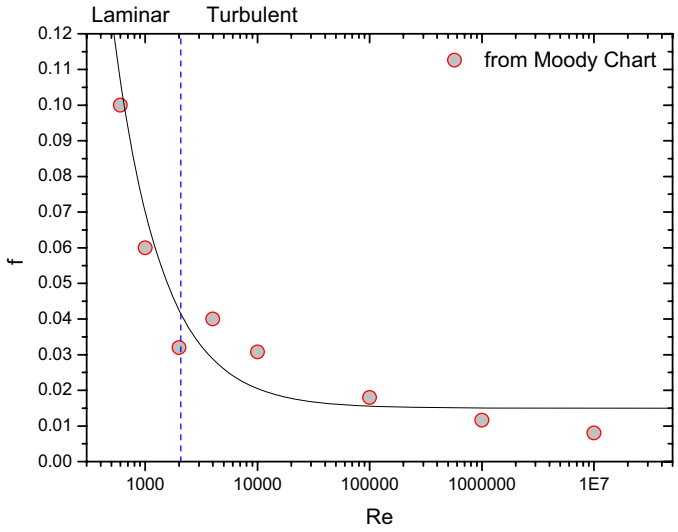

Figure 7. Friction factor as a function of Reynolds number.

To estimate the permeability and inertial resistance, a friction loss correlation (solid line) was fitted to the Moody diagram data as given by Eqn. (9).

$$f = a + \frac{b}{\mathrm{Re}}. \tag{9}$$

Based on Figure 7, the friction factor equation can be correlated as follows.

$$f = 0.015 + \frac{55}{\mathrm{Re}}. \tag{10}$$

The pressure drop correlation is

$$\Delta P = f\left(\frac{1}{2}\rho u^2\right)\left(\frac{L}{D}\right) \tag{11}$$

Inserting Eqn. (10) into Eqn. (11) yields

$$\Delta P = \left(0.015 + \frac{55}{\mathrm{Re}}\right)\left(\frac{1}{2}\rho u^2\right)\left(\frac{L}{D}\right). \quad (12)$$

$$\Delta P = \left(0.015 + \frac{55}{(\rho u D/\mu)}\right)\left(\frac{1}{2}\rho u^2\right)\left(\frac{L}{D}\right). \quad (13)$$

$$\frac{\Delta P}{L} = \frac{55}{2D^2}\mu u + \frac{0.015}{D}\left(\frac{1}{2}\rho u^2\right). \quad (14)$$

Therefore, the permeability (α) and inertial resistance (C_2) are

$$\alpha = \frac{2}{55}D^2, \quad (15)$$

$$C_2 = \frac{0.015}{D}. \quad (16)$$

Since the channel diameter in the core is 0.0158 m, the permeability and inertial resistance are 0.00000908 m^2 and 0.949 m^{-1} respectively. The permeability and the inertia resistance in the core, x-direction can be assumed to be zero and infinite, respectively, as the horizontal flow is negligible in the reactor core.

B. Lower plenum: The porous media parameters in the vertical direction of the lower plenum were determined in the same method as the reactor core. Since the hydraulic diameter in the lower plenum is 0.46 m, the permeability and inertial resistance were calculated to be 0.00769 m^2 and 0.0326 m^{-1} respectively.

The flow resistance in the x-direction of the lower plenum must include the cross flow through the tube array. Figure 8 shows the flow and tube nomenclature.

Figure 9 shows several well known data sets for crossflow. A correlation between the friction factor and the data as a function of Reynolds number is given by the curve fit (solid line).

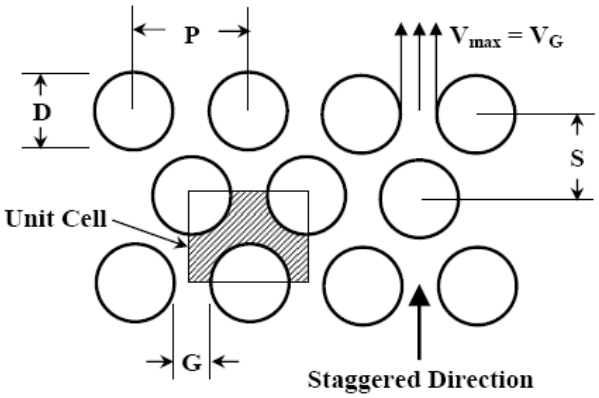

Figure 8. Equally spaced triangular tube array.

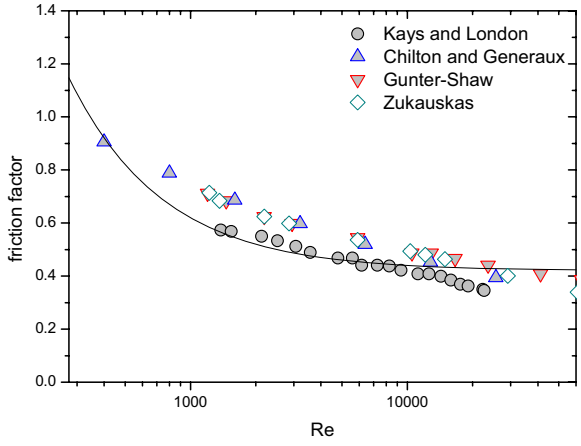

Figure 9. Cross-flow friction factor as a function of Reynolds number.

The friction factor can be correlated as shown in Eqn. (17).

$$f = 0.42 + \frac{200}{\mathrm{Re}} \quad (17)$$

which enables the pressure loss correlation to be expressed by Eqn. (18):

$$\frac{\Delta P}{L} = \frac{100}{D^2}\mu u + \frac{0.42}{D}\left(\frac{1}{2}\rho u^2\right). \quad (18)$$

Therefore, the permeability and inertial resistance are calculated as 0.002116 m^2 and 0.913 m^{-1} respectively.

The permeability of the lower plenum y-direction was determined in the same manner as the core. However, since the lower plenum geometry must consider flow moving parallel to columns, instead of within channels such as occur in the core, the lower plenum hydraulic diameter was

used as the basis to estimate the permeability. The hydraulic diameter of the lower plenum (equals 0.46 m) was calculated using a standard approach based on four times the flow area divided by the wetted perimeter. Using the approach summarized above, the permeability is 0.00668 m^2.

IV. RESULTS

The initial temperature distribution boundary conditions in the lower plenum, bottom reflector, and the core were calculated using the GAMMA systems analysis code [17]. Because the currently-available software cannot calculate the density-gradient driven stratified flow condition, the present calculations only consider diffusion as the driving mechanism for moving air into the reactor vessel.

Figure 10 shows the temperature distributions during the initial 500 seconds following a postulated pipe break. The depressurization phase was completed by 200 sec when momentum-driven flow transitioned to density-gradient-driven stratified flow. Stratified flow was sustained for approximately 100 s (until 300 s into the scenario) when an air-helium mixture was pooled in the bottom of the lower plenum. Subsequently, movement of the air-helium mixture into the reactor core was driven by a combination of diffusion and heating of the gases in the lower plenum. Future studies will include for the relative pressure differences between the reactor cavity and the reactor vessel as a function of their respective pressure distributions.

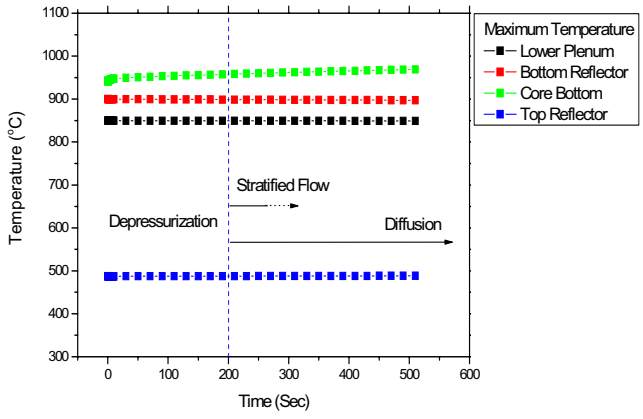

Figure 10. Transient temperature profile.

Based on the calculated results displayed in Fig. 10, the material temperature boundary conditions for the reactor core and other structures were prescribed for the CFD calculations.

Figure 11 shows the variation of air mole fractions in the reactor cavity (Zone 5 in Figure 3) and inside the reactor vessel (Zone 1, 2, 3 and 4) assuming the structures are 1300 K and using the k-ε realizable turbulent model [12]. The initial temperature of the cavity (Zone 5) was assumed to be 300 K. In the lower plenum, the flow was rapidly mixed by additional eddy viscosity terms, so the result shows a flattened air concentration profile along the core axis. Therefore, when the core heating effect is considered, the selection of viscous model will significantly affect the air distributions in the reactor core.

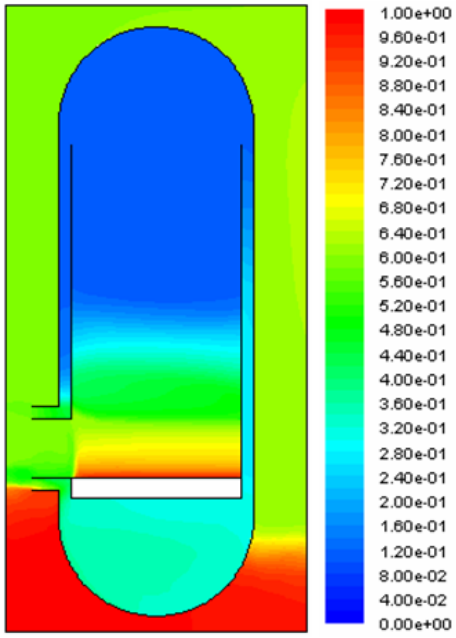

Figure 11. Air distribution in the reactor with initial reactor temperature of 1300 K at 290 seconds.

Figure 12 shows the detailed distribution of the air mole fractions at the center of the reactor calculated using FLUENT as shown in Figure 11. FLUENT was used to model the reactor surrounded by the cavity as shown In Figure 11. At representative structural temperatures, the viscous model affects the air distribution pattern in the reactor. As the temperature increases, the amount of air ingress into the core increases from the expansion of air. When cold air ingresses into the reactor, it is heated by the heated structures and expanded proportional to the inverse of temperature. The lower density air moves upward into the core through the bottom reflector. However, this expansion effect is nearly constant because of no significant density changes when the temperature is greater than 1300 K.

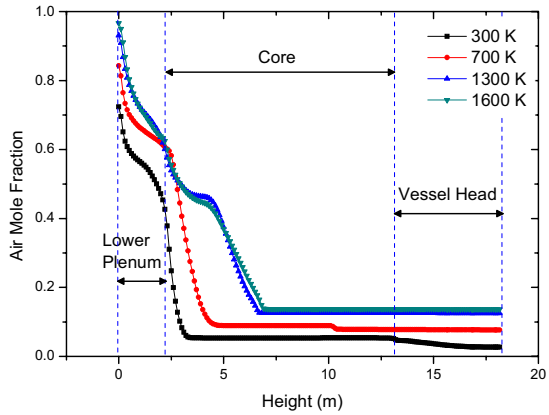

Figure 12. Air distribution at the center of the reactor core after stratified flow process (k-ε realizable model).

V. CONCLUSIONS

A FLUENT CFD model was developed to study the implications of density-difference driven stratified flow on air ingress subsequent to the depressurized conduction cooldown scenario for a GT-MHR 600 MW (thermal) reactor. The calculations imply that density-gradient countercurrent stratified flow will occur following a hypothetical LOCA. Further, stratified flow will result in the movement of air into the reactor vessel much more rapidly than diffusion and thus deserves rigorous study.

The preliminary calculations shown demonstrate the need for a rigorous experimental program to provide validation data to be used for definitive CFD calculations and rigorous studies in the future.

ACKNOWLEDGMENTS

This work was supported through the Department of Energy's Republic of Korea/United States International Energy Research Initiatve (research grant started in FY-08) under DOE Idaho Operations Office Contract DE-AC07-99ID13727.

REFERENCES

1. R. Schultz et al., *Next Generation Nuclear Plant Methods Technical Program Plan*, INL/EXT-06-11804, Rev 0.26, September 2006.

2. General Atomics Co., *Fort Saint Vrain Final Safety Analysis Report*, 1976.

3. General Atomics Co., *Gas Turbine-Modular helium Reactor (GT-MHR) Conceptual Design Description Report* 910720, Revision 1, July, 1996.

4. B. Copsey, M. Lecomte, G. Brinlmann, A. Capitaine, and N. Deberne, "The Framatome ANP Indirect-Cycle Very High Temperature Reactor," *ICAPP'0*4, paper no. 4201, Pittsburgh, PA, June 13-17, 2004.

5. D.R. Nicholls, *Status of the Pebble Bed Modular Reactor*, *Nuclear Energy* **39**, No. 4, 2000.

6. C. P. Liou, R. R. Schultz, and Y. Kukita, "Stably Stratified Flow in Closed Conduits," *Proceedings of the 5th International Conference on Nuclear Engineering,* ICONE5-2024, May 25-29, 1997, Nice, France.

7. C. P. Liou, D. L. Parks, R. R. Schultz, and B. G. Williams, "Stratified Flows in Horizontal Piping of Passive Emergency Core Cooling Systems," *13th International Conference on Nuclear Engineering*, ICONE 13-50450, May 16-20, Beijing, China, 2005.

8. T. Takeda, *Air Ingress Behavior during a Primary-pipe Rupture Accident of HTGR*, JAERI-1338, Japan Atomic Energy Research Institute, 1997.

9. T. Takeda, *Mixing Process of a Binary Gas in a Density Stratified Layer*, JAERI-Research 97-061, Japan Atomic Energy Research Institute, 1997.

10. T. Takeda and M. Hishida, 1996, "Studies on Molecular Diffusion and Natural Convection in a Multicomponent Gas System," *International Journal of Heat and Mass Transfer,* 39, Vol. 3, 1996, pp. 527-536.

11. C. H. Oh, C. Davis, L. Siefken, R. Moore, H. C. NO, J. Kim, G.C. Park, J.C. Lee, and W. R. Martin, *Development of Safety Analysis Codes and Experimental Validation for a Very High Temperature Gas-Cooled Reactor*, Final Report, Idaho National Laboratory, INL/EXT-06-01362, March 2006.

12. E. Kim, Hee No, B. Kim, and C. H. Oh, "Estimation of Graphite and Mechanical Strength Variation of VHTR during Air-Ingress Accident," In press to *Nuclear Engineering and Design*, 2007.

13. E. Kim, Hee No, B. Kim, and C. H. Oh, "Estimation of Graphite and Mechanical Strength Variation of

VHTR during Air-Ingress Accident," In press to *Nuclear Engineering and Design*, 2007.

14. H.C. No. H.S. Lim, J. Kim, C.H. Oh, L. Siefken, and C. Davis, "Multi-component diffusion analysis and assessment of GAMMA code and improved RELAP5 code, *Nuclear Engineering and Design*, 237, 2007. pp. 997-1008.

15. R. R. Schultz, S. E. Krusch, G. E. McCreery, H. McIlroy, C. H. Oh, D. S. Lucas, M. T. Farmer, S. W. Lomperski, C. P. Tzanos, W. D. Pointer, T. Y. C. Wei, and C. P. Liou, "Next Generation Nuclear Plant Methods Thermal-Fluids Experiment Plan," INL/EXT -07-13289, September, 2007.

16. C. S. Yih, *Stratified Flows,* Academic Press, 1980.

17. C.H. Oh, C. Davis, L. Siefken, R. Moore, H.C. NO, J. Kim, G.C. Park, J.C. Lee, and W.R. Martin, *Development of Safety Analysis Codes and Experimental Validation for a Very High Temperature Gas-Cooled Reactor*, Final Report, Idaho National Laboratory, INL/EXT-06-01362, March 2006.

18. FLUENT Inc., Lebanon, N.H., *FLUENT 6.3 User's Guide*, 2005.

19. General Atomics Co., Internal Design Review Presentation Material, December 8-12, 1997.

20. National Institute of Science and Technology (NIST) Chemistry Webbook, http://webbook.nist.gov/chemistry/fluid/

21. D.M. McEligot and G..E. McCreery, *Scaling Studies and Conceptual Experiment Designs for NGNP CFD Assessment*, INEEL/EXT-04-02502, 2004.